

## Research Article

# Synthesis of Nickel Nanoparticles Using Ionic Liquid-Based Extract from *Amaranthus viridis* and Their Antibacterial Activity

Habib Ullah<sup>1</sup>, Mohamed Hefnawy<sup>2</sup>, Zaher Abdel Baki<sup>3</sup>

1. Fundamental and Applied Science Department, Universiti Teknologi Petronas, Malaysia; 2. College of Pharmaceutical Chemistry, College of Pharmacy, King Saud University, Riyadh, Saudi Arabia; 3. College of Engineering and Technology, American University of Middle East, Kuwait

The bioactive components of *Amaranthus viridis* were extracted in the present study using 1-ethyl-3-methyl imidazolium acetate [C<sub>3</sub>MIM] Ac and a microwave. The plant extract was used to synthesize nickel nanoparticles (Ni NPs), whose production was validated by UV/Vis spectrophotometry. The nanomaterials were characterized by X-ray diffraction (XRD), Fourier transform infrared (FTIR) spectroscopy, and thermogravimetric analysis (TGA). The morphology was identified using Field Emission Scanning Electron Microscopy (FESEM), while the particle size and zeta potential were examined using Dynamic Light Scattering (DLS). Nickel nanoparticles were utilized for anti-bacterial activity.

## 1. Introduction

Research on nanoparticles is still underway, and they have uses in medication delivery and therapy, among other things. There are several important and varied uses for nickel nanoparticles, including plastic coating, magnetic fluids, catalysis, and the investigation of anti-cancer processes<sup>[1]</sup>. A variety of chemical processes, including radiation, metal salt reduction, electrochemical procedures, and metal evaporation-condensation, have been used in the past to manufacture nickel nanoparticles<sup>[2]</sup>. However, these methods are unstable, time-consuming, and energy-intensive. A novel extraction method based on microwave help has been developed to get over these constraints.

It employs ionic-liquids to decrease the metal particles to nanoparticle size. Non-molecular ionic compositions containing both inorganic and organic ions are referred to as ionic liquids. The interesting physiochemical properties of ionic liquids have been brought to light by their varied spectrum of reactions<sup>[3][4]</sup>. Meanwhile, it's evident that they serve as solvents for the extraction and separation of chemicals found in natural products<sup>[5]</sup>. Three advantages of microwaves are the mechanical function, pressure, and heat effect. The full use of these features throughout the extraction process leads to a rather high extraction efficiency.

*Amaranthus Viridus* is a member of the Amaranthaceae family, which has 900 species and is distributed in most temperate, tropical, and subtropical regions. These are climbers as well as annuals and perennials, with some being shrubs and herbs. *Amaranthus Viridus* is a tiny plant with alternating leaves and green blooms on a woody green stalk. *Amaranthus viridus* possesses anti-oxidant, antibacterial, and anti-cancer properties that make it useful in medicine<sup>[6][7]</sup>.

The development of resistant germs to current antibiotics has become a major global issue. As a result, new bactericides must be introduced<sup>[8][9]</sup>.

In this study, plant extract was utilized in a green synthesis method to create Ni-nanoparticles. Three distinct bacteria were subjected to antibacterial activity using synthesized nanomaterial.

## 2. Experimental

### 2.1. Material

Merck Millipore, Malaysia is the source of both nickel nitrate  $\text{Ni}(\text{NO}_3)_2$  and 1-ethyl-3-methyl imidazolium chloride [C3MIM] Cl. The plant material, *Amaranthus viridus*, was bought in a Pakistani local market. The experiment utilized just distilled water.

### 2.2. Synthesis of nickel nanoparticle

The plant material (*Amaranthus viridus*) was crushed into a powder after being oven dried at 50 degrees Celsius and twice cleaned with distilled water to get rid of any contaminants. The extract was made by combining 5 g of powder with an aqueous ionic liquid solution in a microwave flask and heating it to 60 °C for 20 minutes at 40 watts. After filtering the mixture, a clear extract was produced. Nickel nanoparticles were created by mixing 5 mL of the extract with an aqueous solution of 0.01 mM  $\text{Ni}(\text{NO}_3)_2$  at 50 W for 30 minutes at 60 °C. Following the reaction, the mixture was triple-washed to

get rid of any remaining contaminants before centrifuging it for five minutes at 4,000 rpm. After an hour of vacuum drying at 60°C, the resultant nanoparticles underwent further characterization.

### 2.3. Characterization

The UV spectra of Ni NPs in the 200–800 nm region were obtained using the Shimadzu UV-2401 twin beam instrument.

Using the FTIR Nicolet 5700, USA, attenuated total reflection (ATR) spectra were collected. The nanomaterial was squeezed with a swivel after being put on a diamond crystal.

Using Ni-filtered Cu K- $\alpha$  radiation and an X-ray diffractometer ( $2\theta$ , 10°–80°, at room temperature) (XPERT-PRO), the crystal structure of Ni NPs was determined. This had receiving slits operating at 40 kV and 0.47° divergent. The Scherrer formula was used to calculate the crystal's size.

Thermogravimetric analysis of Ni NPs was performed using Mettler Toledo SDTA 10000, TG, at a heating rate of 100C/min and a temperature range of 50 to 900°C. Zeiss Supra 55VP FESEM equipment operating at 5 kV was utilized to determine the surface morphology of Ni NPs at different magnifications. Prior to picture observation, the nanoparticles were sufficiently coated with gold water to ensure conductivity. The EDX detector was used to evaluate the identical sample.

Using dynamic light scattering, the zeta potential and particle size were ascertained (Malvern DKS). The measurement sample was divided into two neck cuvettes and poured into water.

### 2.4. Anti-bacterial activity

Synthetic nanoparticles were tested against *Aeromonas hydrophilia*, *Staphylococcus aureus*, and *Escherichia coli* to determine their antibacterial activity. The agar diffusion assay was used to evaluate the nanoparticles' antibacterial activity. After being incubated for 24 hours at 37°C, *E. coli*, *S. aureus*, and *A. hydrophilia* were injected into nutritional broth. Petri plates were evenly coated with nutrient agar before being infected with *Staphylococcus aureus*, *Aeromonas hydrophilia*, and *Escherichia coli*. Various amounts of manufactured nanoparticles were added to each filter paper. After that, the plates were incubated for 24 hours at 37°C. Following the incubation time, precise measurements were made of the nanoparticles' inhibitory zones against each of the three corresponding microorganisms.

### 3. Result and discussions

#### 3.1. UV-Vis analysis of Ni NPs

The antibacterial activity of synthetic nanoparticles was evaluated by subjecting them to tests against *Aeromonas hydrophilia*, *Staphylococcus aureus*, and *Escherichia coli*. The antibacterial activity of the nanoparticles was assessed using the agar diffusion test. *E. Coli*, *S. aureus*, and *A. hydrophilia* were added to nutritious broth after being cultured for a whole day at 37°C. Before *Aeromonas hydrophilia*, *Escherichia coli*, and *Staphylococcus aureus* were added, nutritional agar was equally covered on the petri plates. Every filter paper was treated with different concentrations of artificial nanoparticles. Following that, the plates were incubated at 37°C for a full day. After the incubation period, the inhibitory zones of the nanoparticles against each of the three matching bacteria were measured precisely.

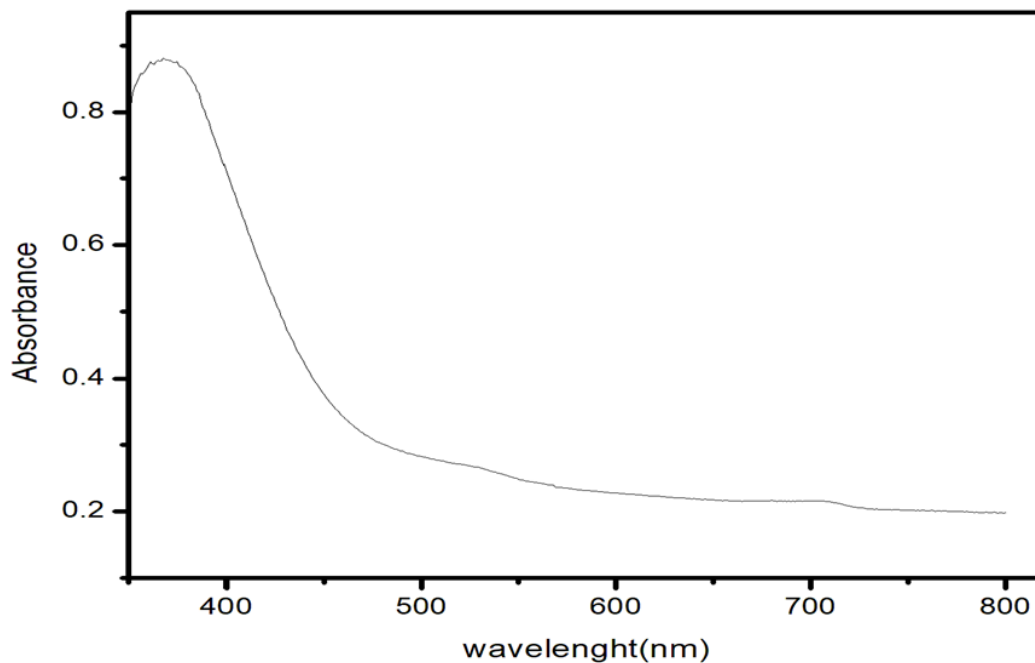


Figure 1. UV/Vis of synthesized Ni nanoparticles

#### 3.2. FTIR analysis

Figure 2 displays the FTIR spectra of Ni NPs both before and after washing. The major wide band in Figure 2 indicates the stretching vibration of OH at 3417 cm<sup>-1</sup>, whereas the band at 1634 cm<sup>-1</sup> is

associated with the bending vibration of O-H bonds. Alkyl groups' C-H stretching and bending vibrations are represented by the bands at 2931  $\text{cm}^{-1}$  and 1378  $\text{cm}^{-1}$ , respectively. The aliphatic amines' C-N stretching vibration is represented by the band at 1080  $\text{cm}^{-1}$ . The aromatic ring's C-C stretching vibrations are represented by the band at 611  $\text{cm}^{-1}$ . These bands show that the plant extract contains flavonoids, aldehyde, amines, and alkane chemicals. These peaks show that the production of Ni NPs and the decrease of nickel ion may be caused by secondary metabolites of the plant. The O-H band's wide width suggested that the Ni NPs were crystalline<sup>[10]</sup>.

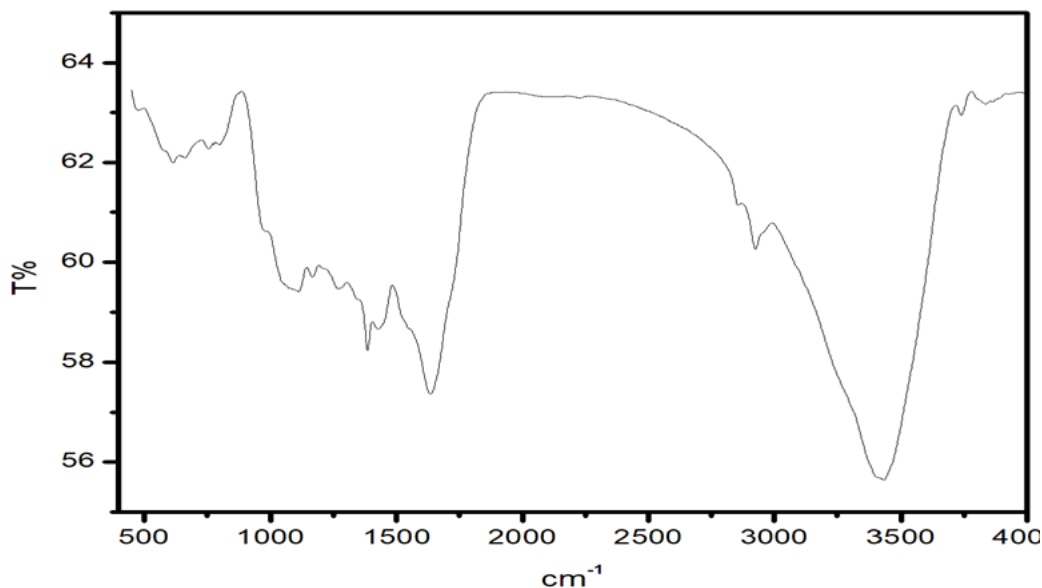


Figure 2. FTIR of Ni nanoparticles

### 3.3. X-rays diffraction analysis (XRD)

The produced Ni NPs' crystalline structure was ascertained using XRD analysis. The Ni NPs XRD pattern is seen in Figure 3. Sharp diffraction strengths at  $2\theta$  values of 33.30, 45.50, and 55.50, which correspond to the crystal planes (100), (111), and (200), in that order. The design indicated a cubic construction with a face in the middle. The diffraction pattern matched the card number 04-0835 in the JCPDS dataset. According to the Debye-Scherrer equation, the crystallite size ranged from 15 to 23 nm<sup>[11][12]</sup>.

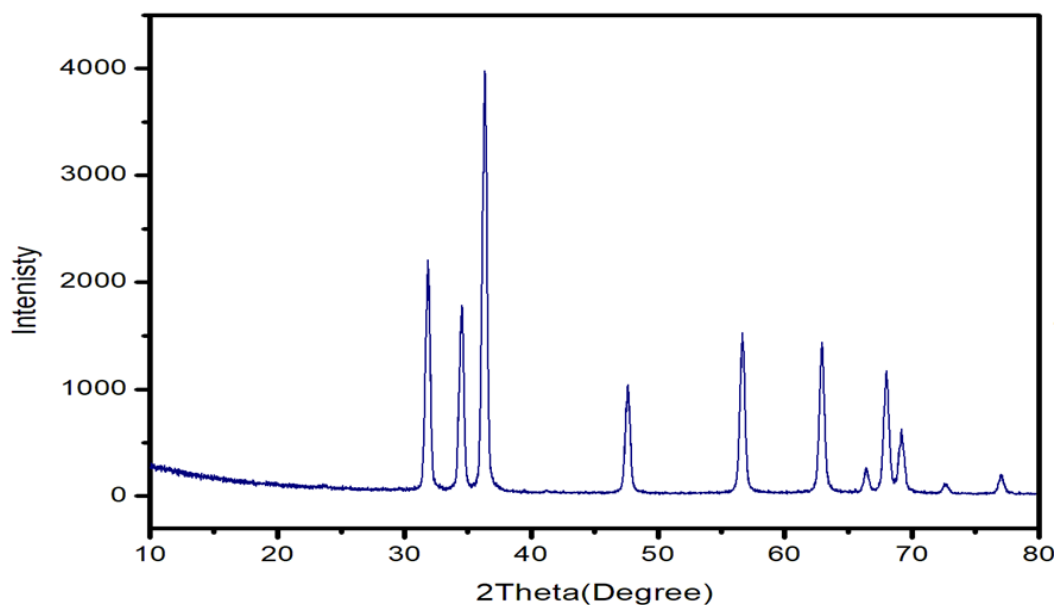


Figure 3. XRD of synthesized Ni nanoparticles

#### 3.4. Thermogravimetric analysis (TGA)

The TGA result for Ni NPs in the 100–500 °C range is displayed in Figure 4. There were three distinct mass losses noted between 100 and 500 °C. In the 100–230 °C regions, the TGA curve indicated a 5% mass loss, which is indicative of a loss of water and less stable molecules. The next mass loss, which accounts for 22% of the mass loss, is seen between 250 and 530 °C and indicates the breakdown of organic molecules. The remaining mass doesn't change beyond 530°C<sup>[13]</sup>.

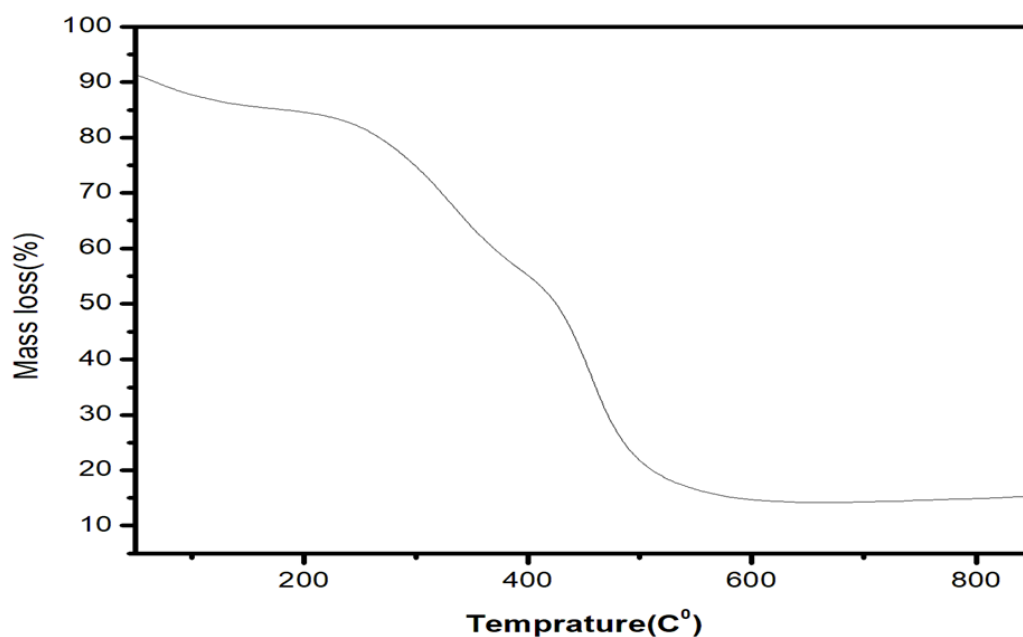


Figure 4. TGA of synthesized Ni nanoparticles

### 3.5. Field emission scanning electron microscopy (FESEM)

The morphology of the nanoparticles may be established with the aid of the FESEM picture. The spherical form of the Ni NPs, measuring between 30 and 55 nm in diameter, is seen in Figure 5(A). The body of available literature provided strong support for the morphology. The fact that there was no agglomeration seen is significant. The sonication cavitation effect may be related to the spherical morphology and agglomeration. Energy dispersive X-ray analysis (EDX) was used to further corroborate the production of pure Ni NPs, as seen in Fig. 5(B). The results of the compositional analysis allowed for a precise measurement of the Ni concentrations. Ni peaks in the EDX spectrum showed that the Ni phase was present and there were no additional impurities<sup>[10][14][15]</sup>.

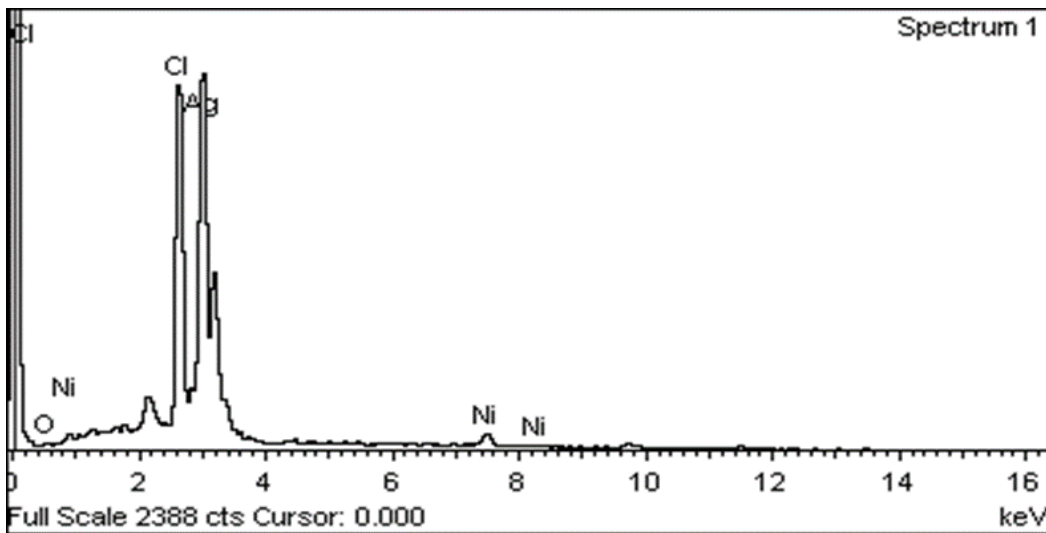
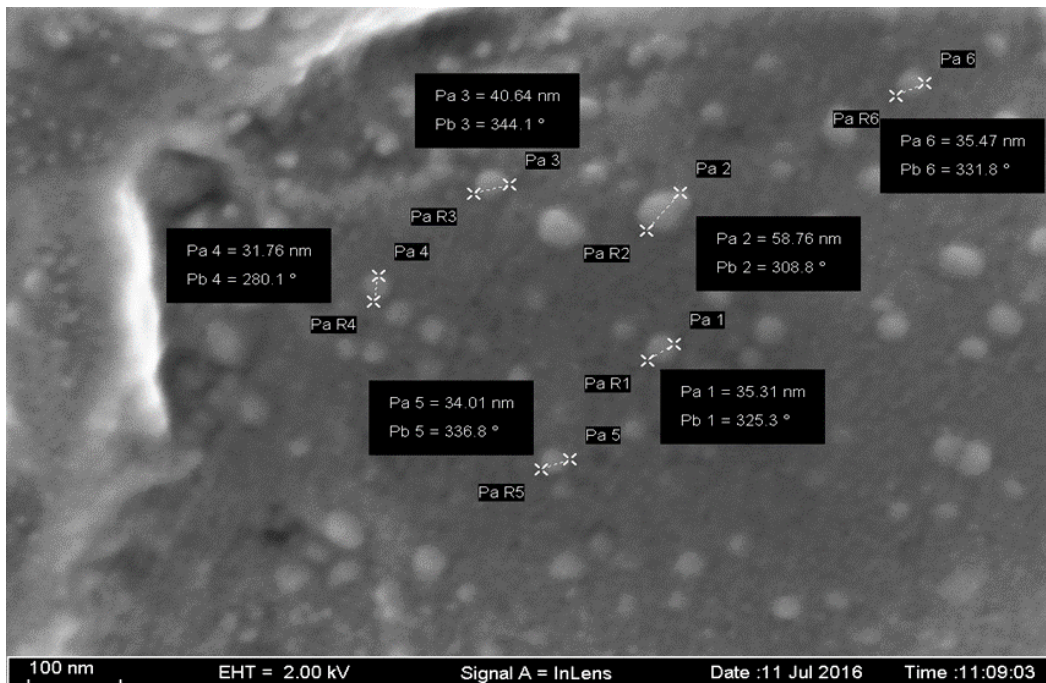
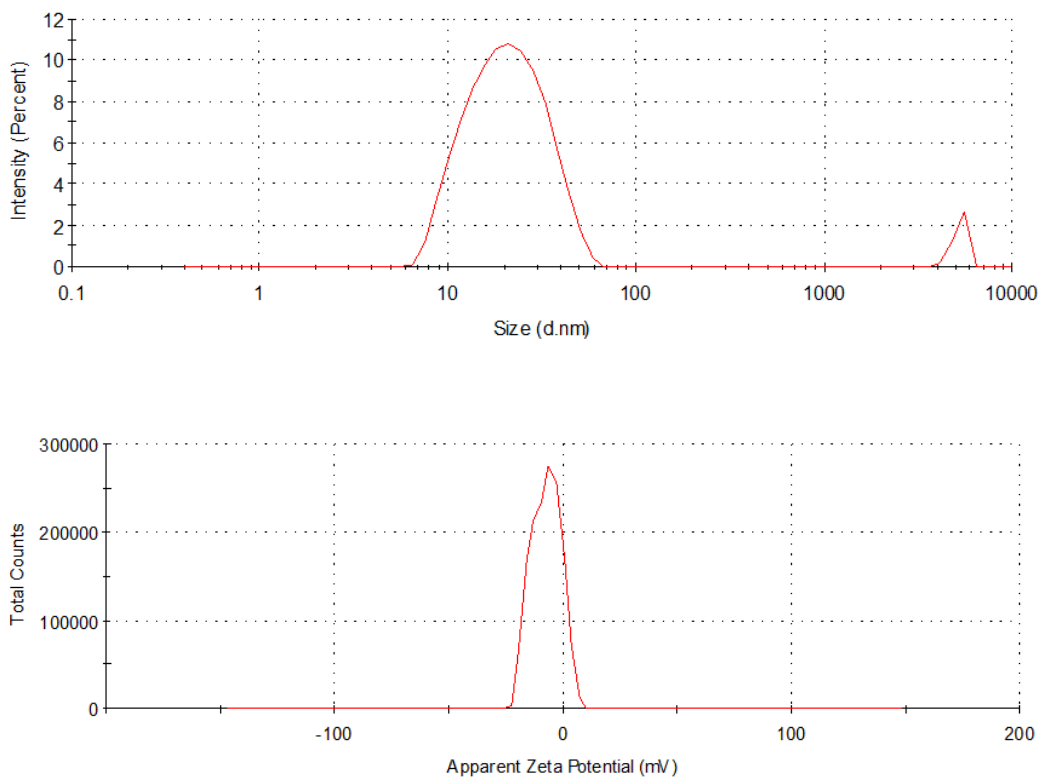


Figure 5. FESEM of synthesized Ni nanoparticles

### 3.6. Zeta size and zeta potential

Figure 6(a) and (b) display the average size and zeta potential of Ni NPs. The produced Ni NPs are polydispersed, with an average diameter of 23.5 nm, according to the particle size peak. Zeta potential is crucial for figuring out a nanoparticle's surface charge and long-term stability. Ni NPs have a zeta

potential of  $-41$  mV on average. The remarkable stability of the nanoparticles is indicated by this value. Thus, a wide range of applications in many sectors are promised by these nanoparticles<sup>[16][17]</sup>.



**Figure 6.** Particles size of synthesized Ni nanoparticles

### 3.7. Anti-bacterial activity

Three distinct gram positive and gram negative bacterial strains were evaluated using the produced Ni NPs ionic liquids-based extract from *Amaranthus viridis*. Figure 7 displays the 10, 20, and 30% zone of inhibition for *Aeromonas hydrophilia*, *Escherichia coli*, and *Staphylococcus aureus*<sup>[18]</sup>. When it comes to combating *Escherichia coli*, Ni NPs outperform *Aeromonas hydrophilia* and *Staphylococcus aureus*. It may be inferred that the nanoparticles demonstrated antibacterial properties. On *Escherichia coli* (16 mm), the highest zone of inhibition was seen at 30%, whereas on *Staphylococcus aureus* and *Aeromonas hydrophilia* (11, 13 mm), the least amount of inhibition was observed<sup>[19][20]</sup>.



Figure 7. Anti-bacterial activity ILMAE based synthesized Ni NPs

## 4. Conclusions

XRD, FESEM, and DLS confirmed that the synthesized nickel nanoparticles (Ni NPs) were nanocrystalline, well dispersed, and deagglomerated. The *Amaranthus viridis* extract, which can be extracted using IL as solvent under microwave treatment, was successfully synthesized using an ionic liquids assisted method. The resulting Ni NPs were 22 nm in size. The synthesized Ni NPs showed zone of inhibition against *Aeromonas hydrophilia*, *Escherichia coli*, and *Staphylococcus aureus*.

## Acknowledgements

The authors extend their appreciation to the Researcher supporting Project number (RSPD2024R754) King Saud University, Riyadh, Saudi Arabia for funding this research.

## References

1. <sup>△</sup>Y. Yuan, J. Rong, L. Zheng, Z. Hu, S. Hu, C. Wu, et al., "Control of the metal-support interactions in Ru on N-doped graphene-encapsulated Ni nanoparticles to promote their hydrogen evolution reaction catalytic performance," *International Journal of Hydrogen Energy*, vol. 52, pp. 687-695, 2024.
2. <sup>△</sup>S. C. Dhawale, A. V. Munde, B. B. Mulik, R. P. Dighole, S. S. Zade, and B. R. Sathe, "CTAB-Assisted Synthesis of FeNi Alloy Nanoparticles: Effective and Stable Electrocatalysts for Urea Oxidation Reactions," *Langmuir*, 2024.

3. <sup>△</sup>K. J. Mohammed, S. K. Hadrawi, and E. Kianfar, "Synthesis and Modification of Nanoparticles with Ionic Liquids: a Review," *BioNanoScience*, vol. 13, pp. 760–783, 2023.
4. <sup>△</sup>Y. Zhang, C. Liu, J. Wang, S. Ren, Y. Song, P. Quan, et al., "Ionic liquids in transdermal drug delivery system: Current applications and future perspectives," *Chinese Chemical Letters*, vol. 34, p. 107631, 2023.
5. <sup>△</sup>X. Li, K. Chen, R. Guo, and Z. Wei, "Ionic liquids functionalized MOFs for adsorption," *Chemical Reviews*, vol. 123, pp. 10432–10467, 2023.
6. <sup>△</sup>J. G. Zorrilla, D. M. Cárdenas, C. Rial, J. M. Molinillo, R. M. Varela, M. Masi, et al., "Bioprospection of Phytotoxic Plant-Derived Eudesmanolides and Guaianolides for the Control of *Amaranthus viridis*, *Echinochloa crus-galli*, and *Lolium perenne* Weeds," *Journal of Agricultural and Food Chemistry*, 2024.
7. <sup>△</sup>G. Bora, S. Gogoi, P. Bora, S. Rahman, and J. Deka, "Evaluation of Promising Lines of Vegetable Amaranth (*Amaranthus viridis* L.) Suitable for Cultivation in North Eastern India," *International Journal of Plant & Soil Science*, vol. 36, pp. 98–102, 2024.
8. <sup>△</sup>A. Yasin, T. Hussain, U. Shuaib, F. E. Mubarik, M. Amjad, S. Ahmad, et al., "Alcoholthermal Synthesis and Characterization of Chitosan Supported Nickel Cobaltite Composite for Enhanced Photocatalytic and Antibacterial Activity," *BioNanoScience*, pp. 1–11, 2024.
9. <sup>△</sup>S.-B. Ghaffari, M.-H. Sarrafzadeh, M. Salami, and A. Alvandi, "A comparative study of the action mechanisms and development strategies of different ZnO-based nanostructures in antibacterial and anticancer applications," *Journal of Drug Delivery Science and Technology*, vol. 91, p. 105221, 2024.
10. <sup>△</sup><sub>b</sub>C. A. Paul, E. R. Kumar, J. Suryakanth, and A. Abd El-Rehim, "Structural, microstructural, vibrational, and thermal investigations of NiO nanoparticles for biomedical applications," *Ceramics International*, 2023.
11. <sup>△</sup>M. W. Alam, A. BaQais, T. A. Mir, I. Nahvi, N. Zaidi, and A. Yasin, "Effect of Mo doping in NiO nanoparticles for structural modification and its efficiency for antioxidant, antibacterial applications," *Scientific Reports*, vol. 13, p. 1328, 2023.
12. <sup>△</sup>N. A. Mala, M. A. Dar, M. u. D. Rather, B. A. Reshi, S. Sivakumar, K. M. Batoo, et al., "Supercapacitor and magnetic properties of NiO and manganese-doped NiO nanoparticles synthesized by chemical precipitation method," *Journal of Materials Science: Materials in Electronics*, vol. 34, p. 505, 2023.
13. <sup>△</sup>K. Motene, L. Mahlaule-Glory, N. Ngoepe, M. Mathipa, and N. Hintsho-Mbita, "Photocatalytic degradation of dyes and removal of bacteria using biosynthesised flowerlike NiO nanoparticles," *International Journal of Environmental Analytical Chemistry*, vol. 103, pp. 1107–1122, 2023.

14. <sup>^</sup>R. Prabhu, N. Jayarambabu, N. Anitha, P. Jitesh, B. Hitesh, and T. V. Rao, "Size dependent electrochemical properties of green synthesized NiO nanoparticles as a supercapacitor electrode," *Inorganic Chemistry Communications*, vol. 160, p. 111836, 2024.
15. <sup>^</sup>M. Momtaz, E. Momtaz, M. A. Mehrgardi, F. Momtaz, T. Narimani, and F. Poursina, "Preparation and characterization of gelatin/chitosan nanocomposite reinforced by NiO nanoparticles as an active food packaging," *Scientific Reports*, vol. 14, p. 519, 2024.
16. <sup>^</sup>Z. H. Athab, A. F. Halbus, A. J. Atiyah, S. S. M. Ali, and Z. Al Talebi, "High-performance photocatalytic degradation and antifungal activity of chromium-doped nickel oxide nanoparticles," *Analytical Sciences*, pp. 1-16, 2024.
17. <sup>^</sup>S. J. Abdulkareem, D. Jafari-Gharabaghlu, M. Farhoudi-Sefidan-Jadid, E. Salmani-Javan, F. Toroghi, and N. Zarghami, "Co-delivery of artemisinin and metformin via PEGylated niosomal nanoparticles: potential anti-cancer effect in treatment of lung cancer cells," *DARU Journal of Pharmaceutical Sciences*, p. 1-12, 2024.
18. <sup>^</sup>Y. Abdallah, S. O. Ogunyemi, F. Wang, H. Xuan, X. Shi, J. Jiang, et al., "Nickel oxide nanoparticles: A new generation nanoparticles to combat bacteria *Xanthomonas oryzae* pv. *oryzae* and enhance rice plant growth," *Pesticide Biochemistry and Physiology*, p. 105807, 2024.
19. <sup>^</sup>L. Yadeta Gemachu and A. Lealem Birhanu, "Green synthesis of ZnO, CuO and NiO nanoparticles using Neem leaf extract and comparing their photocatalytic activity under solar irradiation," *Green Chemistry Letters and Reviews*, vol. 17, p. 2293841, 2024.
20. <sup>^</sup>B. Malini, P. Prashanth, G. Prashanth, and R. Pruthviraj, "Green Synthesis of Undoped and Ag-Doped NiO Nanoparticles: Evaluation and Their Synergetic Effect on Antimicrobial, Anticancer, and Antioxidant Activities," *Anticancer, and Antioxidant Activities*.

## Declarations

**Funding:** The authors extend their appreciation to the Researcher supporting Project number (RSPD2024R754) King Saud University, Riyadh, Saudi Arabia for funding this research.

**Potential competing interests:** No potential competing interests to declare.